Pharmacological Reports
https://doi.org/10.1007/s43440-023-00477-1

SHORT COMMUNICATION

Inhibitory effect of atomoxetine on Nav1.2 voltage-gated sodium channel currents

Yoshihiko Nakatani[1] · Kanami Ishikawa[1] · Yuko Aoki[1] · Takahiro Shimooki[1] · Naoki Yamamoto[1,2,3] · Taku Amano[4]

Received: 18 December 2022 / Revised: 3 March 2023 / Accepted: 5 March 2023
© The Author(s) under exclusive licence to Maj Institute of Pharmacology Polish Academy of Sciences 2023

Abstract

Background Atomoxetine (ATX), a norepinephrine reuptake inhibitor (NRI), is used to attenuate the symptoms of Attention Deficit/Hyperactivity Disorder (AD/HD) by increasing neurotransmitter concentrations at the synaptic cleft. Although Nav1.2 voltage-gated sodium channels (VGSCs) are thought to play a role in monoamine transmitter release in the synaptic junction, it is unclear how atomoxetine affects Nav1.2 VGSCs.

Methods In this study, we investigated the effect of ATX on Nav1.2 VGSC-transfected HEK293 cells with the whole-patch clamp technique.

Results Nav1.2 VGSC current decreased by 51.15 ± 12.75% under treatment with 50 μM ATX in the resting state (holding membrane potential at – 80 mV). The IC_{50} of ATX against Nav1.2 VGSC current was 45.57 μM. The activation/inactivation curve of Nav1.2 VGSC currents was shifted toward hyperpolarization by 50 μM ATX. In addition, the inhibitory effect of ATX increased with membrane depolarization (holding membrane potential at – 50 mV) and its IC_{50} was 10.16 μM. Moreover, ATX showed the time-dependent interaction in the inactivation state.

Conclusion These findings suggest that ATX interacts with Nav1.2 VGSCs producing the inhibition of current and the modification of kinetic properties in the state-dependent manner.

Keywords Atomoxetine · HEK293 · Nav1.2 VGSCs

Abbreviations

NRI	Norepinephrine reuptake inhibitor
AD/HD	Attention deficit/hyperactivity disorder
VGSCs	Voltage-gated sodium channels
NET	Norepinephrine transporter
DAT	Dopamine transporter
ATX	Atomoxetine

✉ Yoshihiko Nakatani
ynakatani@iuhw.ac.jp

1 Department of Pharmacotherapeutics, School of Pharmacy, International University of Health and Welfare, 2600-1 Kitakanemaru, Ohtawara, Tochigi 324-8501, Japan

2 Center for Basic Medical Research, International University of Health and Welfare, 2600-1 Kitakanemaru, Ohtawara, Tochigi 324-8501, Japan

3 Laboratory of Neurobiology, Tokyo Metropolitan University, 1-1 Minami-Osawa, Hachioji-Shi, Tokyo 192-0397, Japan

4 Tochigi Prefectural Okamotodai Hospital, 2162 Shimookamotomachi, Utsunomiya, Tochigi 329-1104, Japan

Introduction

Atomoxetine (ATX) is the first non-stimulant antipsychotic drug approved for the treatment of Attention Deficit/Hyperactivity Disorder (AD/HD) in adults [1]. ATX is considered to improve various symptoms in AD/HD, such as impairments of modulating attention, working memory, behavioral inhibition, planning alertness, arousal, and vigilance, by increasing the concentration of norepinephrine at the synaptic cleft though inhibiting the function of norepinephrine transporters (NET) in the prefrontal cortex. Moreover, there is no risk of addiction with ATX since it does not block dopamine transporters (DAT) of the reward system in the substantia nigra pars compacta and ventral tegmental area [2]. Thus, ATX shows a high affinity for NET with a K_i value of 5 nM, whereas its affinity for the dopamine transporter (DAT) is much lower (K_i value for DAT: 1450 nM) [3]. However, since typical plasma concentrations of ATX at the time of therapeutic treatment (1–3 μM) are high compared to K_i values of ATX to NET or DAT calculated from in vitro experiments [4], the interaction of ATX at the time

Published online: 14 March 2023

of therapeutic treatment may not be restricted to NET and DAT alone.

Nav1.2 voltage-gated sodium channels (VGSCs), which are highly expressed in neurons in the brain, contribute action potential to initiation [5]. Thus, a change, such as gain-of-function or loss-of-function, of Nav1.2 may lead to various symptoms induced by the dysfunction of neuronal excitability in the central nervous system, as typified by epilepsy [6, 7]. Therefore, it considered that the functional modulation of Nav1.2 VGSCs function may affect the release of neurotransmitters including norepinephrine. In addition, it has been reported that ATX interacted with Nav1.5 VGSCs in a state- and use-dependent manner [8]. According to the studies mentioned above, it is possible that Nav1.2 may be an as-yet unknown target for ATX in the therapeutic condition in which its plasma concentration rises above the K_i value of NET.

In this study, we investigated the effect of ATX on the Nav1.2 VGSCs using HEK293 cells transfected with the rat SCN2A gene encoding Nav1.2 VGSCs.

Materials and methods

Establishment and culture of Nav1.2 VGSCs expressing HEK293 cells

The establishment of Nav1.2-expressing HEK293 cells and the culture protocol have been described previously [9]. In brief, the cDNA of Nav1.2 VGSCs inserted into pCI-neo Mammalian Expression Vector (Promega, Fitchburg, WI, U.S.A.) was transfected with FuGENE® 6 Transfection Reagent (Promega) into HEK293 cells (JCRB Cell Bank, Osaka, Japan). Cells expressing Nav1.2 VGSCs were then selected with media containing 500 μg/mL Geneticin (Nacalai Tesque, Inc., Kyoto, Japan). In general, cells were passaged once every 5–7 days.

Electrophysiology

Whole-cell VGSC currents were recorded as described previously with some slight modifications [9]. For electrophysiological experiments, cells that had been cultured 1–4 days from passage on poly-L-lysine-coated cover glass (AGC Techno Glass Co., Ltd., Shizuoka, Japan) were used. In general, culture media containing 500 μg/mL Geneticin was changed every other day to maintain the cell condition. All experiments were performed at 22–25 °C in a bath solution containing (mM) 140 NaCl, 0.03 $CaCl_2$, 10 HEPES, 10 $MgCl_2 \cdot 6H_2O$ and 10 d-glucose, and the pH was adjusted to 7.4 with NaOH. The microelectrode solution consisted of (mM) 115 $CsCl_2$, 25 NaCl, 2 $MgCl_2 \cdot 6H_2O$, 1 $CaCl_2$, 11 EGTA and 10 HEPES, and the pH was adjusted to 7.4 with CsOH. The patch microelectrodes for recording were made from borosilicate capillary glass (Narishige, Tokyo, Japan) and had resistances of 3–5 MΩ. Whole-cell currents were recorded at 50 kHz after low-pass filtering at 3 kHz using EPC-7 Plus and EPC-8 amplifiers (HEKA Elektronik, Lambrecht, Germany) and digitized with Digidater1322A and 1440A (Molecular Devices, Sunnyvale, CA, USA). Leak currents were subtracted by a P/4 pulse protocol. These recorded data were sampled and analyzed using pCLMAP10.6 software (Molecular Devices).

ATX was purchased (Tokyo Chemical Industry Co., Ltd., Tokyo, Japan) and dissolved in DMSO as a stock solution. The final concentration of DMSO in the bath solution was set at 0.1%. To explore the effect of ATX on Nav1.2 VGSC currents, the bath was perfused with a bath solution in which ATX was dissolved at the indicated concentrations.

Data analysis

Data were analyzed using a combination of pCLAMP 10.6 software, Origin 6.1, Microsoft Excel, and GraphPad InStat 3 software. The results are presented as the mean ± SD. For a single comparison of paired data, a statistical analysis was performed using paired *t*-test. A p-value < 0.05 was considered to be statistically significant.

Results

Interaction of atomoxetine with the resting state

First, we investigated the effect of atomoxetine on Nav1.2 VGSCs peak current in the resting state (holding membrane potential at – 80 mV). Figure 1A shows the effect of 50 μM ATX on the Nav1.2 VGSC peak current evoked by depolarization from a holding potential of − 80 mV to a testing potential of 10 mV in HEK293 cells. Under treatment with 50 μM ATX, the Nav1.2 VGSC peak current decreased by around 50% compared to those before treatment with ATX (Fig. 1A). After ATX was washed out, the Nav1.2 VGSC peak current that had been inhibited by the treatment with ATX was almost restored. Figure 1B shows the current-voltage relationship before and during treatment with 50 μM ATX and after washing out. The inhibitory effect of 50 μM ATX started at around − 20 mV and reached a maximum at 10 mV, after which inhibition persisted with further depolarization potentials (Fig. 1B). Nav1.2 peak VGSC current was decreased by 51.15 ± 12.75% under treatment with 50 μM ATX (Fig. 1B) compared to before treatment. The time course changes of Nav1.2 VGSCs peak current inhibitory effect of 50 μM ATX and reversibility (washing out with bath solution) are shown in Fig. 1C. 50 μM ATX inhibited the

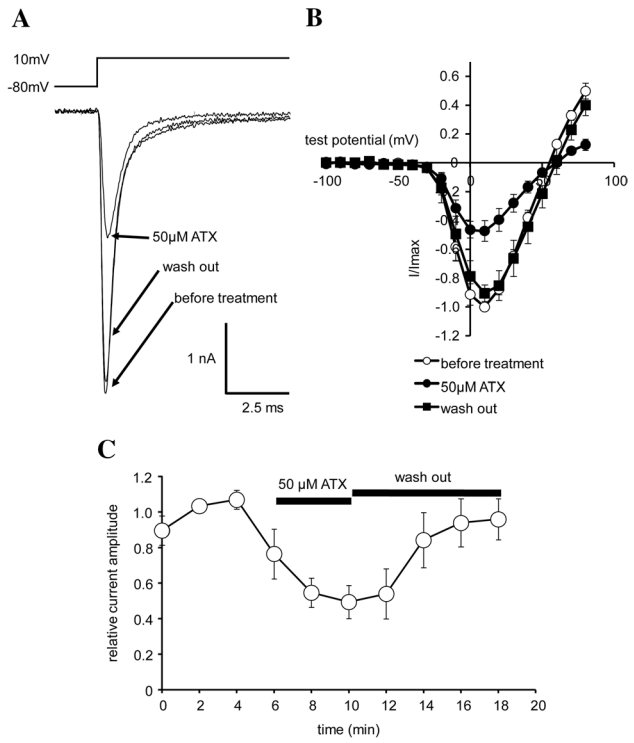

Fig. 1 Effect of ATX on Nav1.2 VGSCs current. (**A**) Current traces recorded from rat Nav1.2 VGSCs expressed HEK293 cells before and after treatment with 50 μM ATX and after washing out of ATX. To record Nav1.2 VGSCs current, cells were held at – 80 mV as holding potential and stepped to a test pulse at 10 mV for 20 ms. (**B**) Current-voltage relationship of normalized Nav1.2 VGSCs current. The normalized peak Nav1.2 VGSCs current before treatment (open circle), under treatment with 50 μM ATX (filled circle) and after washing out of ATX (filled square) were plotted against each depolarizing test potential. Each current-voltage relationship curve is shown as the mean ± SD (n = 6). (**C**) The time course changes of the normalized current amplitude of Nav1.2 VGSCs peak current before and during treatment with 50 μM atomoxetine and after washing out of atomoxetine. The line graph shows mean ± SD (n = 6)

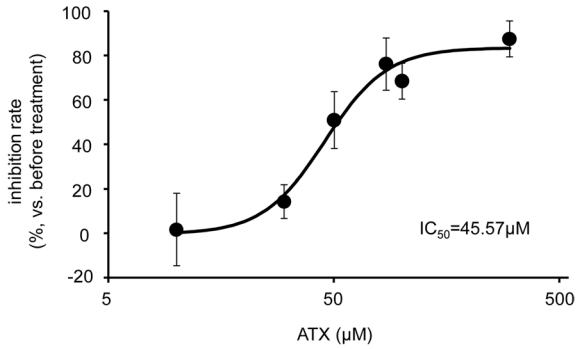

Fig. 2 Concentration-dependent effect of ATX on Nav1.2 VGSCs peak current. Each point on the concentration-response curve represents the mean ± SD (10 μM; n = 7, 30 μM; n = 4, 50 μM; n = 10, 85 μM; n = 4, 100 μM; n = 4, 300 μM; n = 4). The inhibition ratio of ATX at each concentration was fitted using a logistic function; $A_2+(A_1-A_2)/1+(X-Xh)^p$. A_1 *and* A_2 represent the initial value and final value, respectively and X and Xh are the actual concentration and the concentration at which half-maximal inhibition is shown. IC_{50} was determined to be 45.57 μM

Nav1.2 VGSCs peak current gradually, and this inhibition was reversed by washing out ATX with bath solution (Fig. 1C).

Figure 2 shows the concentration-dependent inhibitory effect of ATX on Nav1.2 VGSC peak currents. The inhibition ratio of ATX at each concentration was fitted using a logistic function. Treatment with 10, 30, 50, 85, 100 or 300 μM ATX decreased the Nav1.2 VGSC peak currents by 1.96 ± 16.37%, 14.56 ± 7.57%, 51.15 ± 12.75%, 76.41 ± 11.76%, 68.72 ± 8.05 and 87.72 ± 8.10%, compared to before treatment with ATX, respectively. When the inhibitory effect of Nav1.2 VGSCs peak currents obtained under the treatment with 300 μM ATX was taken to represent as a maximal inhibitory response, IC_{50} was determined to be 45.57 μM.

Effect of atomoxetine in the activation and inactivation

Figure 3A shows the effects of ATX on the activation curves of Nav1.2 VGSCs. To record Nav1.2 VGSC activation current, the cell was held at − 80 mV and stepped to a depolarizing pulse (from − 100 to 30 mV) for 20 ms. The voltage dependence of activation was calculated in two steps. First, changes in driving force in the different test potentials were calculated by the conductance G according to $G=I(E-E_{rev})$. Then, normalized conductance was plotted against the potential of the depolarizing pulse and fitted with the Boltzmann function. The voltage at half-maximal activation changed significantly from − 5.05 ± 3.08 mV to − 9.38 ± 3.30 mV under the treatment with 50 μM ATX (Fig. 3B, n = 6, t_5 = 5.25, p = 0.0033). Figure 3C shows the effects of ATX on the inactivation curves of Nav1.2 VGSCs. To record Nav1.2 VGSCs inactivation current, cells were held at − 80 mV and stepped to an inactivation pulse (from – 100 to 20 mV) for 1 s in steps of 10 mV. Inactivation was determined by plotting the normalized Nav1.2 VGSCs peak current during the following test pulse at – 10 mV for 20 ms versus the pre-pulse potential. The voltage at half-maximal inactivation also changed slightly but significantly from – 50.58 ± 3.18 mV to – 52.64 ± 4.43 mV under the treatment with 50 μM ATX (Fig. 3D, n = 15, t_{14} = 3.38, p = 0.0045).

Interaction of atomoxetine with the inactivating state

Since the inhibitory effect of ATX on Nav1.2 VGSCs peak current in the resting state was relatively small, we assessed

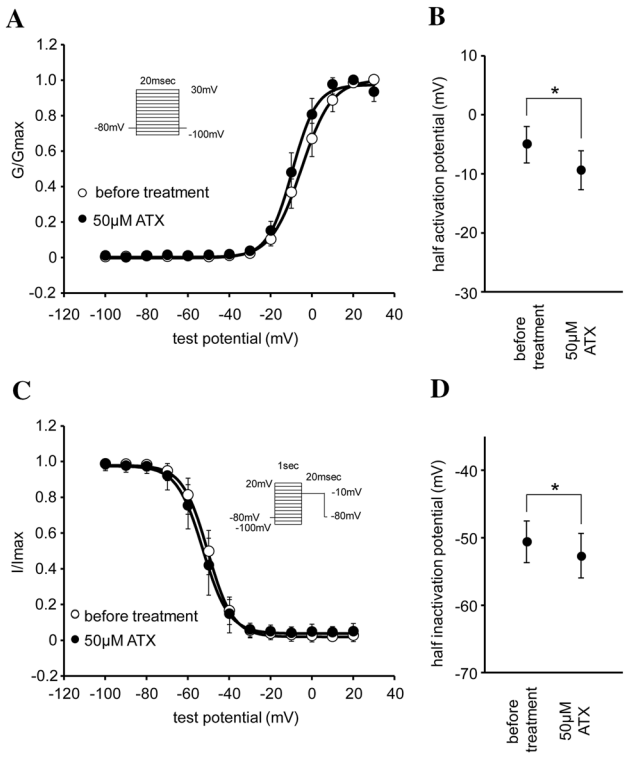

Fig. 3 Effects of ATX on the voltage-dependence of activation and inactivation of Nav1.2 VGSCs. (**A**) Plots of normalized peak conductance (G/G_{max}). These data sets, before (open circle) and after treatment with 50 μM ATX (filled circle), were fitted with a Boltzmann function; $1/1+exp^{((V-Vh)/k)}$. *V* and *Vh* are the actual membrane potential and the potentials at which half-maximal current or conductance are shown. Each activation curve (**A**) and half activation potential (**B**) represent the mean ± SD (n = 6), respectively. To analyze the difference of $V_{1/2}$ in the activation curve between before treatment and 50 μM ATX, a paired *t*-test was performed. (**C**) Plots of normalized inactivation peak currents. These data sets, before (open circle) and after treatment with 50 μM ATX (filled circle), were fitted with a Boltzmann function. Each inactivation curve (**C**) and half inactivation potential (**D**) represent the mean ± SD (n = 15), respectively. To analyze the difference of $V_{1/2}$ in the inactivation curve before treatment and 50 μM ATX, a paired *t*-test was performed

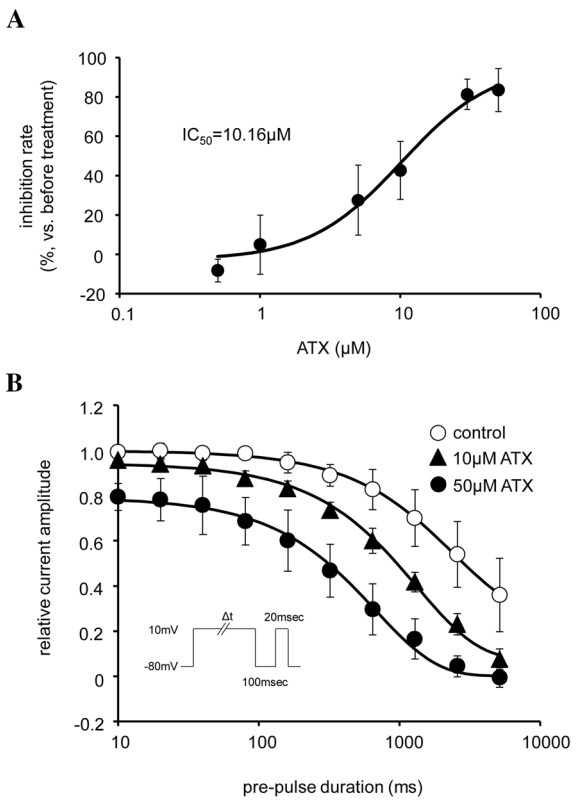

Fig. 4 Effects of ATX on the inactivated state of Nav1.2 VGSCs. (**A**) Concentration-dependent effect of ATX on Nav1.2 VGSCs peak current with holding potential at – 50 mV. Each point on the concentration-response curve represents the mean ± SD (0.5 μM; n = 4, 1 μM; n = 4, 5 μM; n = 5, 10 μM; n = 4, 30 μM; n = 4, 50 μM; n = 4). IC_{50} was determined to be 10.16 μM. (**B**) Time-dependent effect of ATX on Nav1.2 VGSC inactivated state. The peak currents of the test pulse were normalized with the peak currents of conditioning pre-pulse for inactivation and were plotted vs. the duration of conditioning pre-pulse in the absence of ATX (control; open circle), in the presence of 10 μM ATX (filled triangle) and 50 μM ATX (filled circle). These data sets were fitted with single exponential functions. Each point represents the mean ± SD (control; n = 9, 10 μM; n = 5, 50 μM; n = 8)

the effect of ATX on Nav1.2 VGSCs peak current in the inactivated state. The holding membrane potential was chosen to be – 50 mV which is considered the threshold membrane potential in the neuron. Figure 4A shows the concentration-dependent inhibitory effect of ATX on Nav1.2 VGSC peak currents. The inhibition ratio of ATX at each concentration was fitted using a logistic function. Treatment with 0.5, 1, 5, 10, 30 or 50 μM ATX decreased the Nav1.2 VGSC peak currents by – 8.09 ± 5.86%, 5.04 ± 15.07%, 27.59 ± 17.78%, 42.78 ± 14.70%, 81.34 ± 7.71 and 83.64 ± 10.99%, compared to before treatment with ATX, respectively. When the inhibitory effect of Nav1.2 VGSCs peak currents obtained under the treatment with 50 μM ATX was taken to represent a maximal inhibitory response, IC_{50} was determined to be 10.16 μM.

As shown in Fig. 4B, we examined the effect of ATX in the time-dependence interaction with the inactivation state. To assess the time dependence interaction, cells were held at – 80 mV and stepped to an inactivation pulse at 10 mV lasting 10 ms to 5120 ms, followed by a short recovery for 100 ms at – 80 mV and ending with a 20 ms test pulse at 10 mV. The pulse protocol mentioned above was applied in an interval of 20 s. In the absence of ATX, the control values decreased after inactivation pulses lasting longer than 100 ms and dropped to 36.0% ± 14.16% of the conditioning pre-pulse amplitude after the longest inactivation pulse of 5120 ms. In the presence of 10 μM ATX, the decrease of the relative current amplitude of the test pulse to conditioning pre-pulse started in a shorter duration of conditioning pre-pulse with stronger than the absence of ATX (remaining current was 7.57% ± 4.56% at 5120 ms). With the

higher concentration of ATX (50 μM), the inhibitory effect emerged even when conditioning pre-pulse was applied for 10 ms (remaining current: 79.49% ± 5.53%), and the relative current amplitude of conditioning pre-pulse at the longest inactivation time (5120 ms) dropped to – 0.53% ± 4.08% (Fig. 4B).

Tonic and use-dependent block of atomoxetine

To assess the interaction of ATX with the open channel, we examined whether ATX showed a use-dependent block or not. After establishing the baseline condition in the absence of ATX in each cell with the test pulse, bath solution was exchanged to it containing 50 μM ATX and then the test pulse was employed to the cells to activate every 5 s. For evaluation, the peak current amplitude of each pulse was divided by the average of the peak current amplitude obtained from the baseline condition and plotted vs. pulse number. All experiments were performed at the holding potential of − 80 mV and the test pulse was 10 mV for 20 ms. In the absence of 50 μM ATX, the use-dependent behavior was not observed (Fig. 5). When the test pulse was employed to the cells that were pre-treated with 50 μM ATX, it was observed the tonic block by the treatment with 50 μ ATX and the relative current amplitude was decreased to 78.15 ± 4.09% in the first activation with test pulse (Fig. 5). After the test pulse was employed to the cells continuously, the moderate use-dependent block was observed and relative current amplitude was decreased to 59.30 ± 4.41% finally (Fig. 5).

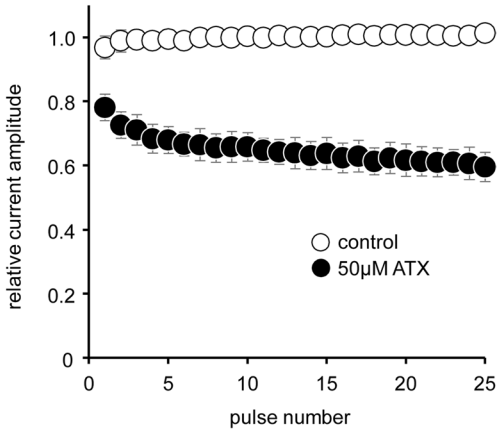

Fig. 5 Use-dependent interaction of ATX on Nav1.2 VGSCs. After establishing baseline current amplitude response, bath solution was exchanged to it containing 50 μM ATX and pre-incubated before the test pulse was applied to the cells. Under control condition (open circle), use-dependence was not observed. In contrast, both tonic and use-dependent blocks were observed in the presence of 50 μM ATX (filled circle). Each point represents the mean ± SD (control; n = 4, 50 μM; n = 4)

Discussion

The present study was designed to update the pharmacological information on ATX which might affect other molecules in the brain other than NET. Our study demonstrated that ATX inhibited resting state Nav1.2 VGSC peak current amplitude in a concentration-dependent manner. In addition, we also clarified that ATX shifted both the activation and inactivation curves of Nav1.2 VGSCs toward hyperpolarization in the resting state. Moreover, when we examined the effect of ATX in the inactivated state of Nav1.2 VGSCs, we found that ATX intensified inhibition of Nav1.2 VGSC peak current amplitude compared to the resting state, and its inhibition was correlated with the length of inactivated duration. In addition, ATX induced both tonic and use-dependent blocks on the Nav1.2 VGSCs peak current amplitude.

A recent study demonstrated that ATX also inhibited Nav1.5 VGSC currents, which are predominantly expressed in the myocardium, with a relatively low concentration at 3 μM [8]. Considering that the calculated IC_{50} of ATX for the Nav1.2 VGSC peak current in our study was 45.57 μM in the resting state, and 10.16 μM in the inactivated state (the holding potential at – 50 mV), it might be concluded that the affinity of ATX for Nav1.5 VGSCs is greater than that for Nav1.2 VGSCs. However, this inhibitory effect of ATX on Nav1.5 VGSC currents was observed when the holding potential was set at – 85 mV, which is approximately the half-maximal inactivated condition. Indeed, the same study also reported that 3 μM ATX could decrease Nav1.5 VGSC currents by only 12.8% and the half-maximal inhibitory effect of ATX on Nav1.5 VGSC currents was 119 μM in the resting state when the holding potential was set at – 140 mV [8]. Considering that ATX showed both tonic and use-dependent block on Nav1.2 VGSCs current amplitude, the inhibitory effect of ATX on Nav1.2 VGSCs may be more potent than that of ATX for Nav1.5 VGSCs in the resting state.

It has been reported that the plasma concentration level of ATX in therapeutic dose application ranges from 1–3 μM [10]. However, the concentration of ATX in brain tissue after single or repeated treatment is not known yet. Considering that the plasma concentration of ATX tends to elevate after chronic treatment in some patients [4, 11] and the IC_{50} of ATX for Nav1.2 VGSCs in the inactivated state was around 10 μM and its value is not so far from the plasma concentration range of ATX at the therapeutic condition, it is possible that accumulated ATX inhibits Nav1.2 VGSCs in a state-dependent manner. In this study, we also demonstrated that both the voltage dependence of activation and inactivation were shifted slightly toward the hyperpolarization side in the resting state. However,

these changes may be too little to affect to the physiological aspect at the therapeutic plasma concentration of ATX.

The primary target molecule of ATX through which it exhibits its therapeutic effect in the treatment of AD/HD is considered to be NET, not Nav1.2 VGSCs. Considering that Nav1.2 VGSCs contribute to initiating an action potential, though we first expected that ATX activated Nav1.2 VGSCs, we found that ATX inhibited Nav1.2 VGSCs activation in fact. However, the possibility that inhibition of Nav1.2 VGSCs may contribute to the therapeutic effect of ATX is raised when we integrate the results from several studies. An association between increased pyrethroid pesticide exposure, which might cause abnormalities in the dopamine system, and AD/HD in US children has been reported [12]. Deltamethrin, a pyrethroid pesticide, was shown to prolong sodium channel current in mouse neuroblastoma N1E-115 cells expressing Nav1.2 VGSCs [13, 14]. In addition, single-channel analysis demonstrated that deltamethrin increased the population of long-duration openings, consequently increasing Na^+ selectivity in rat Nav1.2 VGSCs expressed in Xenopus oocytes [15]. Considering these results, it is possible that the activation of VGSCs including Nav1.2 expressed in the central nervous system may be related to the expression of AD/HD symptoms; therefore, the inhibition of Nav1.2 VGSCs by ATX might partially contribute to attenuating symptoms of AD/HD under certain conditions.

There is an apparent contradiction because the inhibition of Nav1.2 VGSC currents induced by ATX theoretically decreases the release of neurotransmitters including norepinephrine at the synaptic cleft although ATX exerts its therapeutic effect in the treatment of AD/HD through an increase in neurotransmitter by inhibiting NET function. However, it has also been shown that loss-of-function of Nav1.2 VGSCs causes epilepsy which is considered to be induced by the excitation of neurons in the brain [6, 16]. In addition, a recent study demonstrated the down-regulation of multiple potassium channels including Kv1.1 followed by enhanced intrinsic neuronal excitability in Nav1.2 VGSC-deficient neurons; therefore, this mechanism may cause epilepsy under loss-of-function of Nav1.2 VGSCs [17]. It has been reported that the sodium channel activator, reduced the expression of sodium channel alpha-subunit mRNA and its reduction was blocked by the treatment of tetrodotoxin, a VGSCs blocker, in developing neurons [18]. Thus, the inhibitory effect of ATX on Nav1.2 for AD/HD treatment is possible to be explained as follows: long-term exposure to ATX that leads to the prolonged inhibition of Nav1.2 VGSCs may change the expression levels of various ion channels including itself on neuronal membrane followed by an increase in membrane excitability to enhance neurotransmitter release. Considering that the plasma concentration of ATX in the therapeutic condition is 1–3 μM or may elevate higher depending on the patient background, it is possible that the function of Nav1.2 VGSCs may be inhibited under certain conditions partially. However, since it remains whether the chronic pharmacological inhibition of Nav1.2 VGSCs affects the expression levels of various types of ion channels in neurons, further examinations will be needed to clear its possibility.

In summary, ATX inhibited Nav1.2 VGSC peak currents in a concentration-dependent manner. This inhibition was more intense in the inactivated state than the resting state of Nav1.2 VGSCs and its inhibition in the inactivation state showed in the time-dependent manner. Moreover, both voltage dependence of activation and inactivation were shifted toward hyperpolarization by treatment with ATX in the resting state. Considering the possible impact of ATX on Nav1.2 VGSCs in neurons, ATX may decrease the activity of Nav1.2 VGSCs in the central nervous system within the brain. Further studies will be needed to clarify whether the correlation between the electrophysiological mechanisms of the inhibitory effect of atomoxetine on Nav1.2 VGSCs contributed to its therapeutic effect.

Acknowledgements We specially thank Dr. Weitemier (Tokyo Metropolitan University) gave constructive advice to refine our manuscript. We also thank the members of the Department of Pharmacotherapeutics, School of Pharmacy, International University of Health and Welfare, for their helpful discussions throughout this study.

Author contribution YN designed this study initially. YN, KI, YA and TS generated experimental data. YN also analyzed experimental data and created figures. YN wrote the manuscript with support from NY and TA.

Funding This work was supported by an internal research grant from International University of Health and Welfare.

Data availability The datasets generated during the current study are available from the corresponding author on reasonable request.

Declarations

Conflict of interest None to declare.

References

1. Christman AK, Fermo JD, Markowitz JS. Atomoxetine, a novel treatment for attention-deficit-hyperactivity disorder. Pharmacotherapy. 2004;24(8):1020–36.
2. Prince J. Catecholamine dysfunction in attention-deficit/hyperactivity disorder: an update. J Clin Psychopharmacol. 2008;28(3 Suppl 2):S39-45.
3. Bymaster FP, Katner JS, Nelson DL, Hemrick-Luecke SK, Threlkeld PG, Heiligenstein JH, et al. Atomoxetine increases extracellular levels of norepinephrine and dopamine in prefrontal cortex of rat: a potential mechanism for efficacy in attention deficit/hyperactivity disorder. Neuropsychopharmacology. 2002;27(5):699–711.
4. Papaseit E, Marchei E, Farré M, Garcia-Algar O, Pacifici R, Pichini S. Concentrations of atomoxetine and its metabolites in plasma and oral fluid from paediatric patients with attention deficit/hyperactivity disorder. Drug Test Anal. 2013;5(6):446–52.

5. Horvath GA, Demos M, Shyr C, Matthews A, Zhang L, Race S, et al. Secondary neurotransmitter deficiencies in epilepsy caused by voltage-gated sodium channelopathies: A potential treatment target? Mol Genet Metab. 2016;117(1):42–8.
6. Menezes LFS, Sabiá Júnior EF, Tibery DV, Carneiro LDA, Schwartz EF. Epilepsy-Related Voltage-Gated Sodium Channelopathies: A Review. Front Pharmacol. 2020;11:1276.
7. Qiao X, Werkman TR, Gorter JA, Wadman WJ, van Vliet EA. Expression of sodium channel α subunits 1.1, 1.2 and 1.6 in rat hippocampus after kainic acid-induced epilepsy. Epilepsy Res. 2013;106(1–2):17–28.
8. Föhr KJ, Nastos A, Fauler M, Zimmer T, Jungwirth B, Messerer DAC. Block of Voltage-Gated Sodium Channels by Atomoxetine in a State- and Use-dependent Manner. Front Pharmacol. 2021;12: 622489.
9. Nakatani Y, Amano T. Functional Modulation of Nav1.2 Voltage-Gated Sodium Channels Induced by Escitalopram. Biol Pharm Bull. 2018;41(9):1471–4.
10. Sugimoto A, Suzuki Y, Orime N, Hayashi T, Egawa J, Sugai T, et al. Non-Linear Pharmacokinetics of Atomoxetine in Adult Japanese Patients With ADHD. J Atten Disord. 2020;24(3):490–3.
11. Garside D, Ropero-Miller JD, Riemer EC. Postmortem tissue distribution of atomoxetine following fatal and nonfatal doses–three case reports. J Forensic Sci. 2006;51(1):179–82.
12. Wagner-Schuman M, Richardson JR, Auinger P, Braun JM, Lanphear BP, Epstein JN, et al. Association of pyrethroid pesticide exposure with attention-deficit/hyperactivity disorder in a nationally representative sample of U.S. children. Environ Health. 2015;14:44.
13. Chinn K, Narahashi T. Stabilization of sodium channel states by deltamethrin in mouse neuroblastoma cells. J Physiol. 1986;380:191–207.
14. Baroni D, Moran O. Molecular differential expression of voltage-gated sodium channel α and β subunit mRNAs in five different mammalian cell lines. J Bioenerg Biomembr. 2011;43(6):729–38.
15. Peng F, Mellor IR, Williamson MS, Davies TG, Field LM, Usherwood PN. Single channel study of deltamethrin interactions with wild-type and mutated rat Na(V)1.2 sodium channels expressed in Xenopus oocytes. Neurotoxicology. 2009;30(3):358–67.
16. Ogiwara I, Miyamoto H, Tatsukawa T, Yamagata T, Nakayama T, Atapour N, et al. Nav1.2 haplodeficiency in excitatory neurons causes absence-like seizures in mice. Commun Biol. 2018;1:96.
17. Zhang J, Chen X, Eaton M, Wu J, Ma Z, Lai S, et al. Severe deficiency of the voltage-gated sodium channel Na. Cell Rep. 2021;36(5): 109495.
18. Lara A, Dargent B, Julien F, Alcaraz G, Tricaud N, Couraud F, et al. Channel activators reduce the expression of sodium channel alpha-subunit mRNA in developing neurons. Brain Res Mol Brain Res. 1996;37(1–2):116–24.

Publisher's Note Springer Nature remains neutral with regard to jurisdictional claims in published maps and institutional affiliations.